Selective oxidation of pyrogallol-type catechins with unripe fruit homogenate of *Citrus unshiu* and structural revision of oolongtheanins

Yosuke Matsuo*, Fumiya Tadakuma, Takuya Shii, Yoshinori Saito, Takashi Tanaka*

Graduate School of Biomedical Sciences, Nagasaki University, Bunkyo-Machi 1-14, Nagasaki 852-8521, Japan

*Corresponding authors: Tel.: +81-95-819-2434 (Y.M.); Tel.: +81-95-819-2432 (T.T.).

E-mail addresses: y-matsuo@nagasaki-u.ac.jp (Y. Matsuo), t-tanaka@nagasaki-u.ac.jp (T. Tanaka).

Graphical Abstract

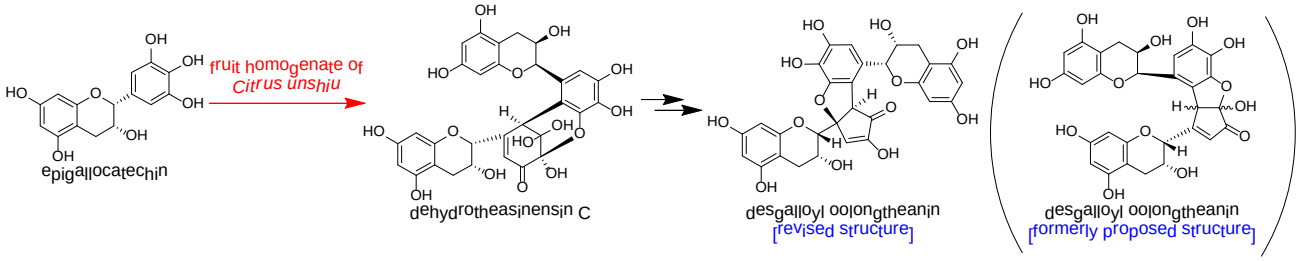

Abstract

In our previous chemical study of the production mechanism of black tea polyphenols, we demonstrated that Japanese pear fruit homogenate oxidizes green tea catechins bearing pyrogallol-type and catechol-type B-rings to produce theaflavins and dehydrotheasinensins. In contrast, unripe fruit homogenate of *Citrus unshiu* selectively oxidizes pyrogallol-type catechins to yield only dehydrotheasinensins. The difference in the selectivity of the two homogenates is probably related to the lower redox potential of pyrogallol-type catechins. The oxidation of epigallocatechin with *C. unshiu* homogenate gave two new compounds, including an ethanol adduct of an oolongtheanin precursor and epigallocatechin 4′-*O*-rutinoside, together with theasinensin C, dehydrotheasinensin E, and desgalloyl oolongtheanin. The structure of desgalloyl oolongtheanin should be revised based on the spectroscopic and computational data collected in the current study, and a mechanism responsible for the production of oolongtheanins is also proposed.

Keywords: Catechin, Oxidation, *Citrus unshiu*, Oolongtheanins, Black tea

1. Introduction

Polyphenols, such as catechins, proanthocyanidins, and caffeoyl esters, are widely distributed throughout the plant kingdom, and are believed to be accumulated as defense substances against herbivores and microorganisms. Polyphenols are usually oxidized by oxygen with the aid of enzymes when plants are physically damaged or harmed by predators. This process generally involves the reduction of oxygen molecules to generate reactive oxygen species, such as the superoxide anion and hydrogen peroxide, which not only act as defensive molecules but also behave as signaling molecules to trigger other defense mechanisms.[1] However, the oxidation products of polyphenols have not been thoroughly characterized to date. Black tea is produced by the mechanical crushing of the fresh leaves of *Camellia sinensis*. During this process, the four major tea catechins (**1**–**4**, Fig. 1) are oxidized by enzymes originally localized in different tissues of the leaf to give a complex mixture of black tea polyphenols.[2] Although a large number of the oxidation products in black tea have been identified, including theaflavins,[3] theasinensins (**8**–**10**),[4,5] oolongtheanins (**11**, **15**, **16**),[5] and theacitrins,[6] more than half of the total polyphenols present in a black tea infusion remain uncharacterized.[2a,7] The mechanisms responsible for the production of individual black tea polyphenols also remain ambiguous. To develop a better understanding of the oxidation products and the reaction mechanisms responsible for their formation, we have shown that the in vitro oxidation of single catechin components or a pair of catechins with various enzyme sources is effective for obtaining sufficient amounts of the oxidation products for spectroscopic characterization.[8,9] The products resulting from the treatment of tea catechins with some plant homogenates, such as Japanese pear and loquat, were

found to be closely related to those produced by tea leaf enzymes.[9] However, a significant difference in the enzyme specificity was observed for the unripe fruit homogenates of *Citrus unshiu*.[10] In this study, we initially examined the oxidation of tea catechins with the unripe fruit homogenates of *C. unshiu* and characterized the resulting products by spectroscopic methods. The structures of oolongtheanins (**11**, **15**, **16**), which belong to a group of polyphenols found in oolong tea and black tea, were also reinvestigated in the current study using spectroscopic and computational methods,[11] and a novel mechanism is proposed for the degradation of dehydrotheasinensins (**5**–**7**) leading to production of oolongtheanins.

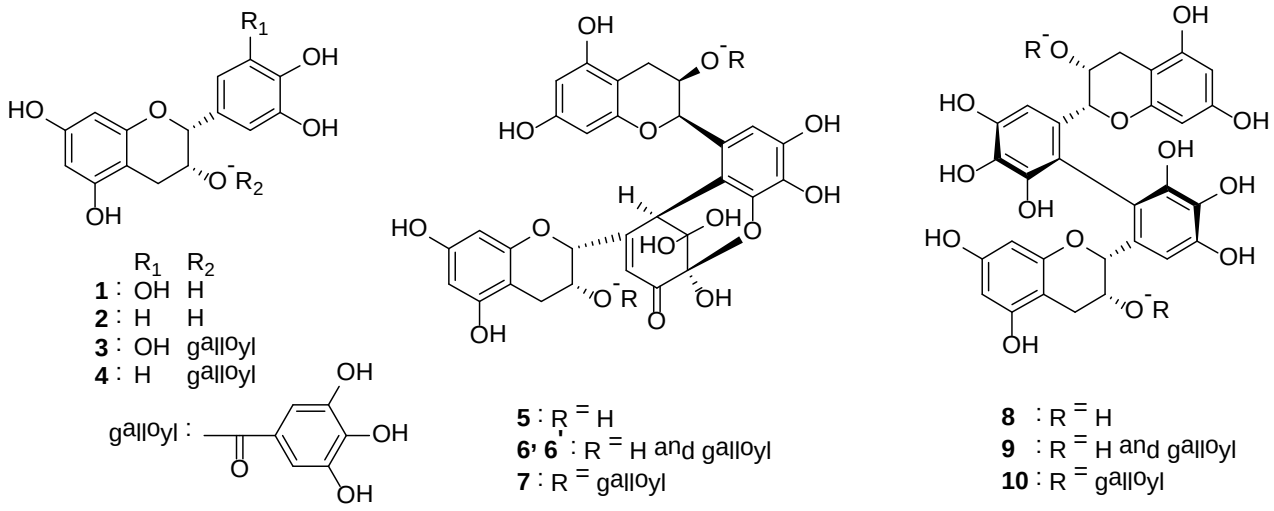

Fig. 1. Structures of tea catechins **1**–**4**, dehydrotheasinensins **5**–**7**, and theasinensins **8**–**10**.

2. Results and discussion

2.1. Oxidation of catechin mixture with plant homogenates.

The oxidation of a mixture of tea catechins (Fig. 2a) with Japanese pear homogenates produced

theaflavins and theasinensins (**8**–**10**) (Fig. 2b and Supplementary Data). Theaflavins are directly produced by the oxidative coupling of catechol-type catechins [(−)-epicatechin (**2**) and its galloyl ester (**4**)] with pyrogallol-type catechins [(−)-epigallocatechin (**1**) and its galloyl ester (**3**)].[3,12] In contrast, theasinensins are produced by the reduction of unstable intermediates known as dehydrotheasinensins **5**–**7**, which are themselves generated by oxidative dimerization of pyrogallol-type catechins.[13] The Japanese pear homogenate oxidized both the catechol-type and pyrogallol-type B-rings to produce both theaflavins and dehydrotheasinensins (**5**–**7**). In contrast, the unripe fruit homogenate of *Citrus unshiu* oxidized only **1** and **3** to compounds **5**–**7** (Fig. 2c). This difference in the selectivity of the homogenates is probably related to the lower redox potential of the pyrogallol-type catechins compared with the catechol-type catechins.[14] Subsequent treatment of the reaction mixture with ascorbic acid generated theasinensins **8**–**10** (Fig. 2d). In this experiment, compounds **5**–**7** were reduced with ascorbic acid to avoid unnecessary complexity in the products. During the actual process of black tea production, the dehydrotheasinensins undergo an oxidation‐reduction dismutation process,[13b,c] which results in the production of theasinensins as the reduction products and oolongtheanins and many other uncharacterized compounds as the oxidation products (see Supplementary Data).

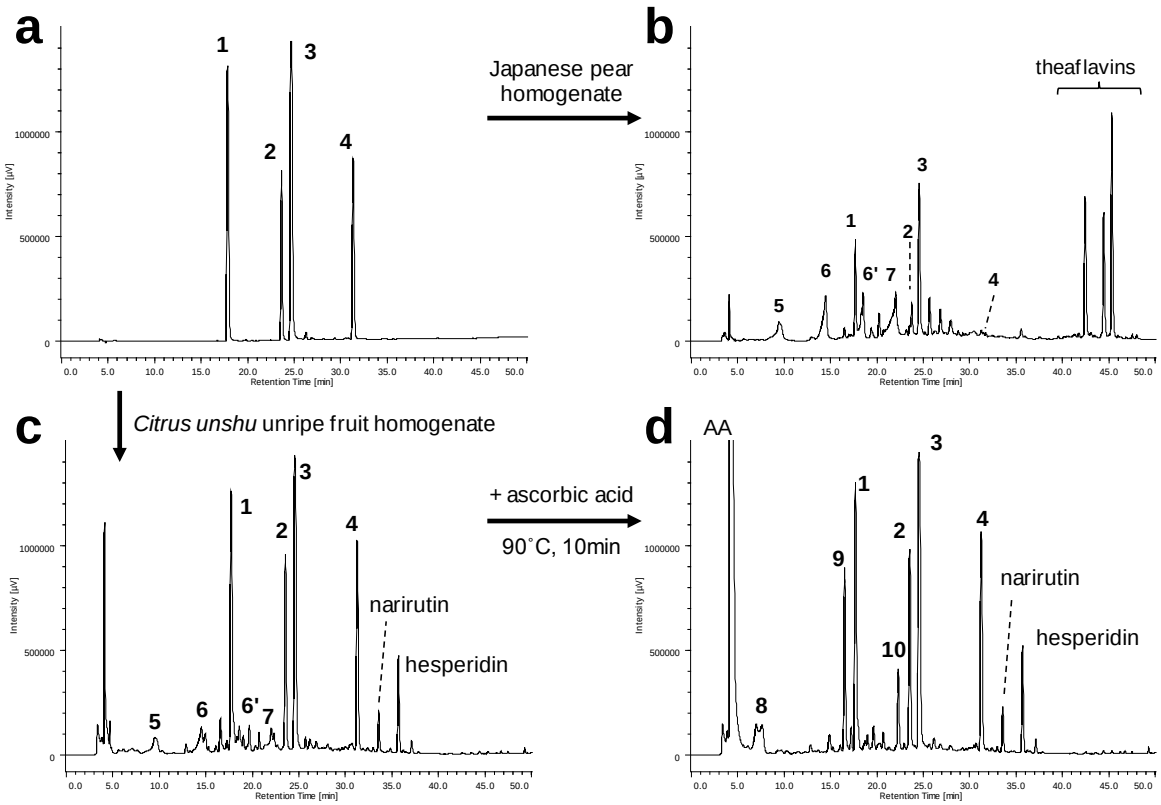

Fig. 2. HPLC chromatograms of the tea catechin mixtures treated with fruit homogenates. **a** Tea catechin mixture consisting of (−)-epigallocatechin (**1**), (−)-epicatechin (**2**), (−)-epigallocatechin-3-*O*-gallate (**3**), and (−)-epicatechin-3-*O*-gallate (**4**). The proportion of the catechins was based on the concentrations found in Japanese green tea leaves. **b** After treatment with the Japanese pear fruit homogenate. Peaks **5**–**7** are dehydrotheasinensins. **c** After treatment with the unripe fruit homogenate of *Citrus unshiu*. Hesperidin and narirutin originated from the homogenate. **d** After heating the reaction mixture shown in **c** with ascorbic acid (AA) (90 °C, 10 min). Peaks **8**–**10** are theasinensins.

We then performed a large-scale oxidation of (−)-epigallocatechin (**1**) with the unripe fruit homogenate of *C. unshiu* to examine the reaction in greater detail. An aqueous solution of **1** was vigorously stirred with the unripe fruit homogenate of *C. unshiu*. The reaction was terminated with

the addition of ethanol, and the products were purified by column chromatography to afford theasinensin C (**8**) (about 39%), desgalloyl oolongtheanin (**11**)[5] (2.2%), dehydrotheasinensin E (**14**)[9] (0.9%), and two new products **12** (1.8%) and **13** (0.2%) (Fig. 3). Analysis of the initial reaction mixture by HPLC indicated that dehydrotheasinensin C (**5**) had been produced as the major product. Interestingly, however, theasinensin C (**8**), which is the reduction product of **5**, was obtained as the major product after column chromatography. In addition to the reduction of **5** to **8** by the ascorbic acid originally contained in the fruit homogenate, compound **5** also underwent an oxidation–reduction dismutation process when it was concentrated at 40–45 °C and during its subsequent chromatographic separation, which led to the production of **8**.

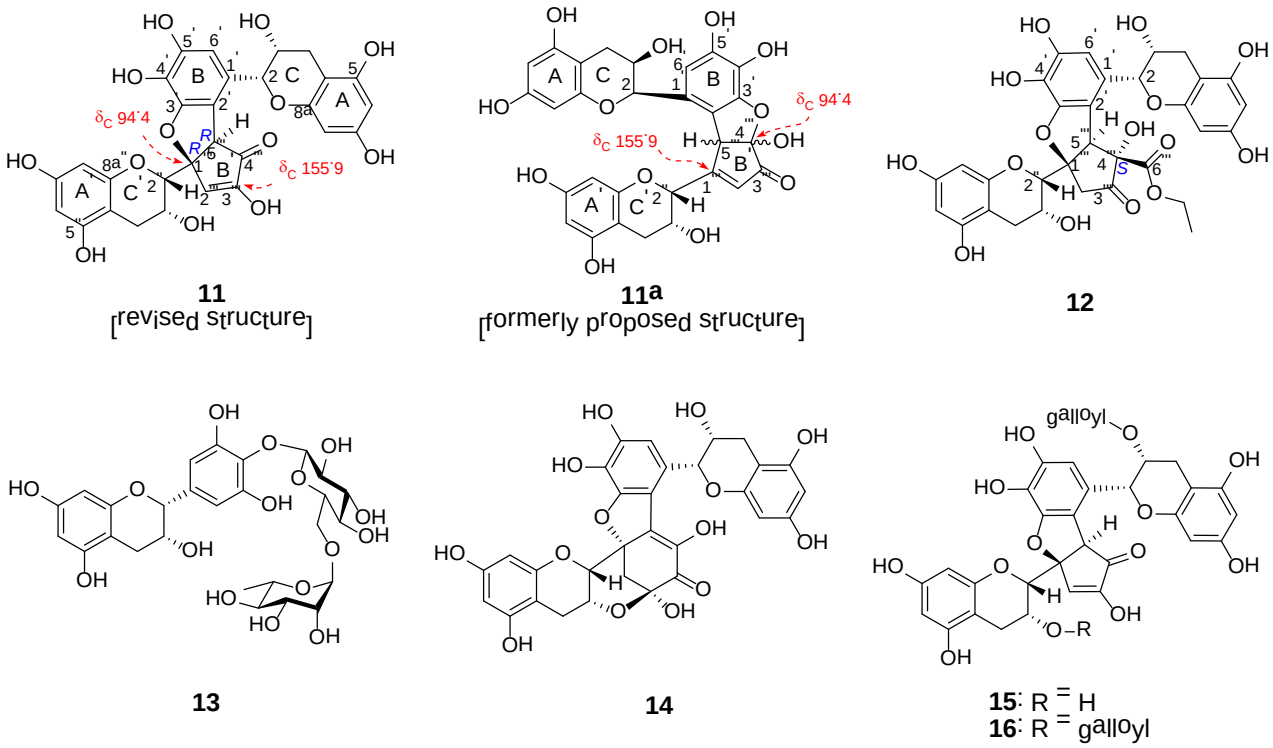

Fig. 3. Structures of products **11**–**16**.

2.2. Structural revision of oolongtheanins

Oolongtheanins—desgalloyl oolongtheanin (**11**), oolongtheanin (**15**), and galloyl oolongtheanin (**16**)—were originally identified as the polyphenols contained in oolong tea and black tea,[5,15] and we previously demonstrated that they are produced by degradation of dehydrotheasinensins.[13b,c] The original structure **11a** was proposed based on its 1D-NMR spectra and methylation derivatization, and its stereochemistry was not established. With this in mind, we re-examined the structure of this compound in the current study. The signals derived from the A-, A′-, C-, and C′-rings of the flavan-3-ol were assigned by ^{1}H-^{1}H COSY, HSQC, and HMBC correlations (Table 1). In addition, the signals belonging to the pyrogallol-type B-ring (C-1′–C-6′) corresponded with those of the proposed structure **11a**, which was confirmed by the appearance of HMBC correlations from H-2 (δ_H 5.14) to C-1′ (δ_C 128.3), C-2′ (δ_C 115.6), and C-6′ (δ_C 109.4), as well as correlations from H-6′ (δ_H 6.90) to C-2 (δ_C 76.6), C-1′, C-2′, C-4′ (δ_C 130.2), C-5′ (δ_C 146.8), and C-3′ (δ_C 147.6, ^{4}J) (Fig. 4). The remaining ^{13}C NMR signals were attributed to a conjugated carbonyl carbon (δ_C 200.2), an sp^2 quaternary carbon (δ_C 155.9), an sp^2 methine (δ_C 124.6), an sp^3 quaternary carbon (δ_C 94.4), and an sp^3 methine (δ_C 53.6). To confirm the location of the free hydroxyl group on the B′-ring, ^{13}C NMR spectra were recorded in acetone-d_6 + H_2O and in acetone-d_6 + D_2O. The resultant chemical shifts were carefully compared because the corresponding C–OH and C–OD moieties gave different chemical shifts.[16] The carbon signal at δ_C 94.4, which was originally assigned to the hemiacetal carbon at C-4‴ bearing a hydroxyl group in **11a**, did not undergo a hydrogen/deuterium exchange reaction. However, the sp^2

carbon signal at δ_C 155.9, which was originally assigned as the C-1‴ carbon in **11a** with no hydroxyl group, did show an apparent change in its chemical shift (i.e., $\Delta\delta_C$ 0.107) (Fig. 5). In the original structure **11a**, the strong HMBC correlation from H-2″ (δ_H 4.32) through four covalent bonds to the hemiacetal carbon with a signal at δ_C 94.4 was unlikely. Taken together with the strong HMBC correlation from the C-ring H-2″ to the signals at δ_C 53.6 (C-5‴) and δ_C 124.6 (C-2‴), these results allowed for the planar structure of desgalloyl oolongtheanin to be revised to the structure shown as formula **11**.

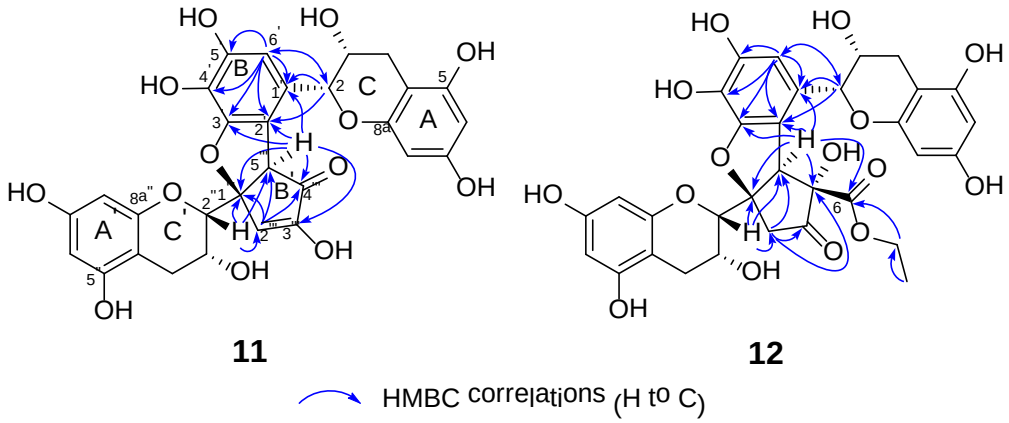

Fig. 4. Selected HMBC correlations for **11** and **12**.

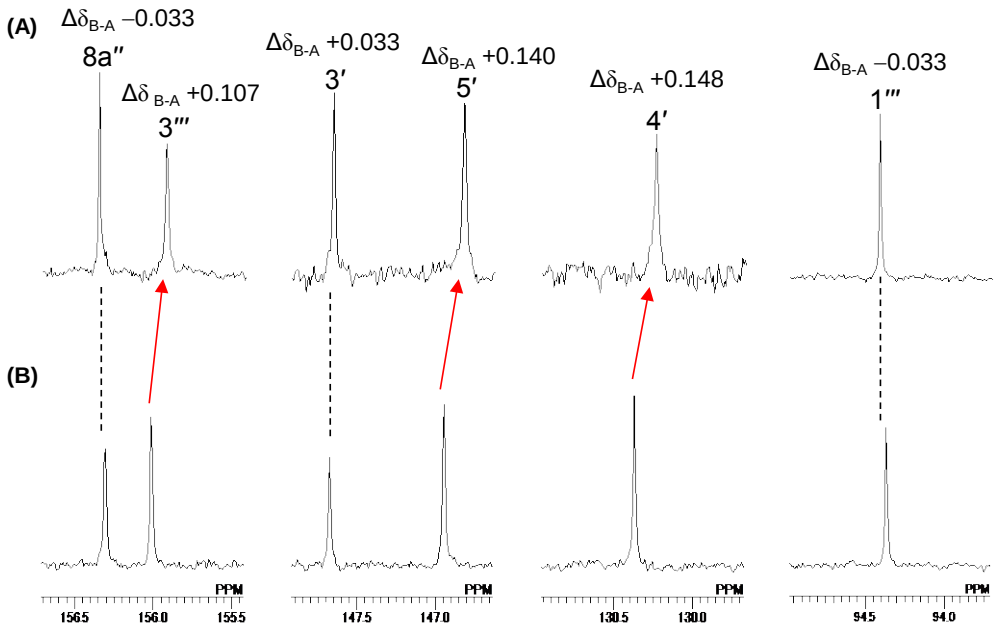

Fig. 5. Hydrogen‑deuterium exchange shifts in the ^{13}C NMR spectra of **11**. **A** Selected signals from the ^{13}C NMR spectrum of **11** measured in acetone-d_6 + D_2O (95:5; v/v); **B** Selected signals from the ^{13}C NMR spectrum of **11** measured in acetone-d_6 + H_2O (95:5; v/v).

Table 1. ^{1}H (500 MHz) and ^{13}C (125 MHz) NMR data for **11** and **12** (in acetone-d_6 – D_2O, 95:5 – v/v).

position		**11**			**12**		
		^{1}H[a]	^{13}C	HMBC (H to C)	^{1}H[a]	^{13}C	HMBC (H to C)
C	2	5.14 (s)	76.6	3, 4, 1', 2', 6'	4.85 (s)	77.4	3, 4, 8a, 1', 2', 6'
	3	3.99 (m)	65.7	4a	4.35 (m)	65.6	2, 4, 4a
	4	3.03 (dd, 16.4, 4.5)	29.5	2, 3, 4a, 5, 8a	2.88 (dd, 16.3, 4.3)	30.0	2, 3, 4a, 5, 6 (^{4}J), 8 (^{4}J), 8a, 1' (^{4}J)
		2.77 (br d, 16.4)			2.77 (br d, 16.3)		
A	4a		99.6			99.6	
	5		157.1 [b]			157.7 [f]	
	6	5.99 (d, 2.4)	96.0	4a, 5, 7, 8	5.99 [d] (d, 2.3)	96.1 [g]	4a, 5, 7, 8
	7		157.5 [c]			157.6 [f]	
	8	5.82 (d, 2.4)	95.4	4a, 6, 7, 8a	5.85 [d] (d, 2.3)	95.5 [g]	4a, 6, 7, 8a
	8a		157.5			157.4 [f]	
B	1'		128.3			128.7	
	2'		115.6			117.2	
	3'		147.6			148.9	
	4'		130.2			130.0	
	5'		146.8			147.3	
	6'	6.90 (s)	109.4	2, 1', 2', 3' (^{4}J), 4', 5', 5''' (^{4}J)	6.95 (s)	109.5	2, 1', 2', 3' (^{4}J), 4', 5', 5''' (^{4}J)
C'	2''	4.32 (s)	78.8	3'', 4'', 1''', 2''', 5'''	3.84 (s)	77.1	3'', 4'', 1''', 2''', 5'''
	3''	4.34 (m)	62.8	4a''	4.65 (m)	61.7	4'', 4a''
	4''	2.72 (2H, m)	29.7	2'', 3'', 4a'', 5'', 8a''	2.78 (br d, 16.3)	29.6	2'', 3'', 4a'', 5'', 6'' (^{4}J), 8'' (^{4}J), 8a'', 1''' (^{4}J
					2.66 (dd, 16.3, 4.3)		
A'	4a''		99.1			99.4	
	5''		157.3 [b]			157.4 [f]	
	6''	5.95 (d, 2.3)	96.2	4a'', 5'', 7'', 8''	5.96 [e] (d, 2.3)	96.4 [h]	4a'', 5'', 7'', 8''
	7''		157.7 [c]			157.2 [f]	
	8''	5.72 (d, 2.3)	95.2	4a'', 6'', 7'', 8a''	5.80 [e] (d, 2.3)	95.3 [h]	4a'', 6'', 7'', 8a''
	8a''		156.3			156.1 [f]	
B'	1'''		94.4			92.3	
	2'''	6.58 (s)	124.6	2'', 1''', 4''', 5'''	3.70 (d, 14.7)	44.3	2'', 1''', 3''', 4''', 5'''
					3.26 (d, 14.7)		
	3'''		155.9			213.1	
	4'''		200.4			85.8	
	5'''	4.52 (s)	53.6	1', 2', 3', 4' (^{4}J), 6' (^{4}J), 2'', 1''', 2''', 3''', 4'''	4.32 (s)	59.3	1', 2', 3', 4' (^{4}J), 6' (^{4}J), 2'', 1''', 2''', 4''', 6'''
	6'''					170.4	
	Ethyl CH_2				3.82 (m)	62.4	6''', Ethyl CH_3
					3.72 (m)		
	Ethyl CH_3				0.95 (3H, t, 7.2)	13.6	Ethyl CH_2

[a] Multiplicities and coupling constants (Hz) have been shown in parentheses. [b–h] May be interchanged in the same column.

The stereostructure of **11** was examined based on the theoretical calculations of its ECD spectrum.[17] Because **11** was derived from **1**, the absolute configurations at C-2, C-3, C-2″, and C-3″ were determined as 2*R*, 3*R*, 2″*S*, and 3″*R*, respectively. This result therefore indicated that there were four possible absolute configurations for the remaining stereocenters, including (1‴*R*,5‴*R*), (1‴*S*,5‴*S*), (1‴*S*,5‴*R*), and (1‴*R*,5‴*S*). Among them, the (1‴*S*,5‴*R*) and (1‴*R*,5‴*S*) configurations would have a *trans*-conjunction of two five-membered rings, which would be unlikely because of the their highly strained structure. With this in mind, we only performed theoretical calculations for the ECD spectra of (1‴*R*,5‴*R*)-**11** and (1‴*S*,5‴*S*)-**11** using TDDFT at the CAM-B3LYP/6-31G(d,p) level in methanol using the polarizable continuum model (PCM), following the conformational search and geometrical optimization. The resulting lowest-energy conformers of (1‴*R*,5‴*R*)-**11** and (1‴*S*,5‴*S*)-**11** are shown in Fig. 6, and the Boltzmann-weighted calculated ECD spectra are shown in Fig. 7. The experimental ECD spectrum of **11** showed a positive Cotton effect at 241 nm, which resembled that of the calculated ECD spectrum of (1‴*R*,5‴*R*)-**11**. In contrast, the calculated ECD spectra of (1‴*S*,5‴*S*)-**11** showed a negative Cotton effect at that region. Taken together, these results indicate that the Cotton effect around 240 nm reflects the configuration of the cyclopentenone moiety of **11**, and the absolute structure of **11** was therefore assigned as the (1‴*R*,5‴*R*) configuration. Based on these data, we were able to successfully revise the structure of desgalloyl oolongtheanin (**11**), as shown in Fig. 3. The structures of its galloyl esters, oolongtheanin (**15**) and galloyl oolongtheanin (**16**) (Fig. 3), should also be revised because **11** was produced by tannase hydrolysis from **15** and **16**.[5] It is noteworthy that the planar structure of **16** is the same as that of an oxidative dimerization product

of epigallocatechin-3-*O*-gallate (**3**), which is produced by an autoxidation reaction in authentic intestinal juice, rat plasma, and bile.[18] With this in mind, we also performed the autoxidation of **3** according to the procedures described in the literature[18b] and confirmed the production of **16** from **3**.

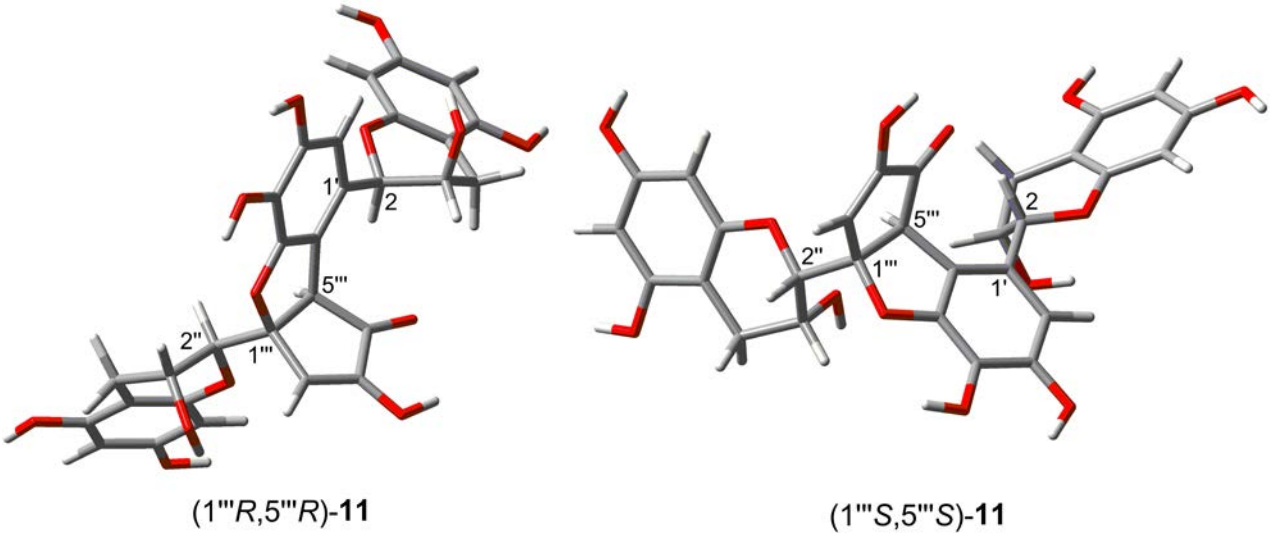

Fig. 6. Lowest-energy conformers of (1‴*R*,5‴*R*)-**11** and (1‴*S*,5‴*S*)-**11**. Geometrical optimization was performed at the B3LYP/6-31G(d,p) level in methanol (PCM).

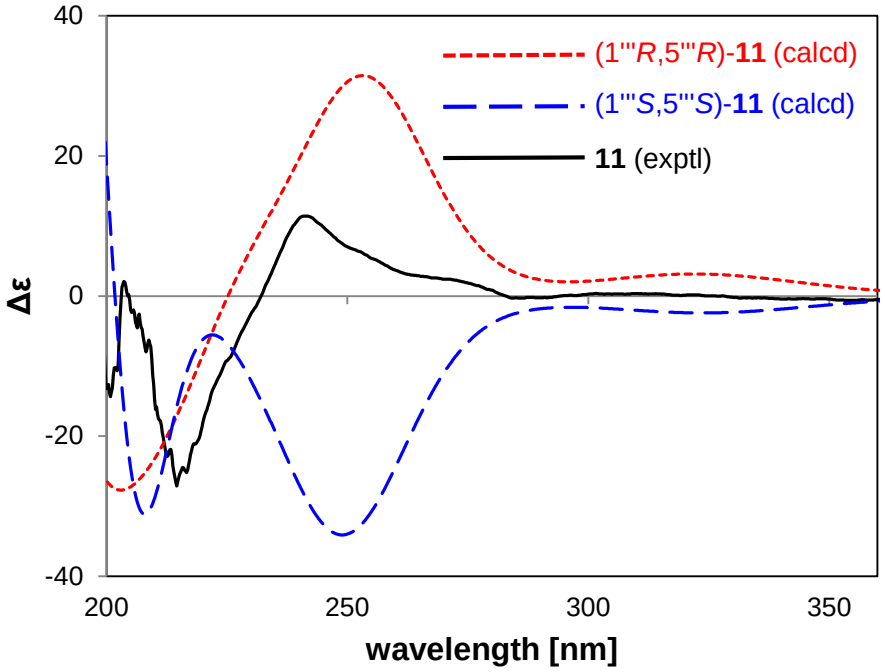

Fig. 7. Experimental and calculated ECD spectra of **11**. The experimental ECD spectrum was measured in methanol. The calculations for the ECD spectra were performed at the TD-CAM-B3LYP/6-31G(d,p) level in methanol (PCM). The calculated spectra were red-shifted by 10 nm.

2.3. Structure of ethanol adduct 12 and proposed production mechanism of oolongtheanins

Analysis of compound **12** by FABMS showed an $[M + H]^+$ peak of *m/z* 655, revealing the compound to be a dimer of **1**. Taken together with its ^{13}C NMR and elemental analysis data, the molecular formula of **12** was assigned as $C_{32}H_{30}O_{15}$. The ^{1}H- and ^{13}C NMR spectra of **12** indicated the presence of a pyrogallol ring (B-ring) and two sets of flavan A- and C-rings, which were similar to those of **11**. The ^{13}C NMR spectrum revealed the presence of a nonconjugated carbonyl (δ_C 213.1, C-3″), a carboxyl (δ_C 170.4, C-6″), two quaternary carbons (δ_C 92.3, C-1‴; δ_C 85.8, C-4‴), a methine (δ_C 59.3, C-5‴), and a methylene (δ_C 44.3, C-2‴) carbon. Furthermore, HMBC correlations (Fig. 4)

revealed that the carboxyl group formed an ethyl ester (δ_H 0.95, 3H, t, CH_3; δ_H 3.72 and 3.82, each 1H, m, CH_2). The remaining HMBC correlations of the methine (H-5‴), methylene (H-2‴), and C-ring H-2 and H-2″ protons indicated the presence of a cyclopentanone ring (C-1‴–C-5‴). The degree of unsaturation was calculated to be 18 based on the molecular formula, while the unusual low-field shift of the C-1‴ signal (δ_C 92.3), which is very similar to that of C-1‴ in **11** (δ_C 94.4), suggested that there was an ether ring between the C-1‴ and pyrogallol C-3′. Thus, the planar structure of **12** was assigned as shown in Fig. 3. The structural relationship between this product and **11** led us to propose a new mechanism for their generation from dehydrotheasinensin C (**5**) (Scheme 1). Compound **12** was produced by the addition of ethanol, which was used to terminate the enzymatic reaction, to the oxidized pyrogallol ring. In contrast, the addition of water to the same oxidized pyrogallol ring followed by decarboxylation afforded an enediol intermediate, and the subsequent oxidation of the enediol produced **11**.[19] This newly proposed mechanism also suggested that the stereostructures of the C-1‴ and C-5‴ positions in **12** were the same as those of **11**. The ^{1}H and ^{13}C NMR chemical shifts of (4‴*S*)-**12** and (4‴*R*)-**12** were calculated to determine the configuration at the C-4‴ position.[20] Low-energy conformers within 6 kcal/mol were initially obtained following a conformational search using the Monte Carlo method at the MMFF94 force field, and these conformers were subsequently optimized at the B3LYP/6-31G(d,p) level in acetone (PCM). The ^{1}H- and ^{13}C NMR chemical shifts of the low-energy conformers with high Boltzmann populations (> 1%) were calculated using the gauge-including atomic orbital (GIAO) at the mPW1PW91/6-311+G(2d,p) level in acetone (PCM). The experimental ^{1}H- and ^{13}C NMR chemical shifts of **12** agreed to a much greater extent with the

calculated values for (4‴*S*)-**12** (correlation coefficient R^2 = 0.9908 for ^{1}H NMR; R^2 = 0.9992 for ^{13}C NMR) than (4‴*R*)-**12** (R^2 = 0.9733 for ^{1}H NMR; R^2 = 0.9979 for ^{13}C NMR) (see Supplementary Data for details). Based on these results, the structure of **12** was assigned as shown in Fig. 3.

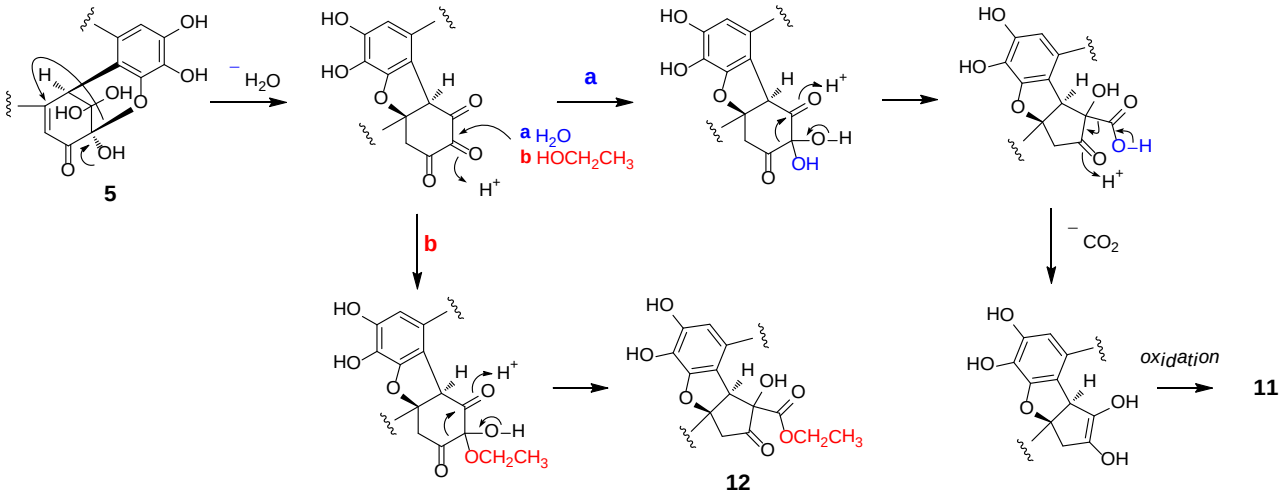

Scheme 1. Plausible mechanisms for the production of **11** and **12**.

2.4. Structure of 13

New compound **13** showed ^{1}H and ^{13}C NMR signals that were consistent with the structure of **1** together with aliphatic signals that could be attributed to two hexose moieties. A comparison of the chemical shifts of compound **13** with those of rutin[21] revealed that **13** was a rutinoside (6-*O*-α-L-rhamnopyranosyl-β-D-glucoside) of **1**. The low-field shift of the glucose C-6 carbon (δ_C 68.2 in CD_3OD) confirmed the location of the rhamnosyl moiety at this position. The composition of the sugars and their absolute configuration were determined by acid hydrolysis followed by HPLC analysis of the thiazolidine derivatives.[22] The sugar moiety was shown to be attached to the C-4′

hydroxyl group of the B-ring, because the B-ring carbon signals were shifted to lower field [e.g., C-4′ (δ_C 138.3, Δδ 5.3), C-3′ and C-5′ (δ_C 150.3, Δδ 4.1), C-1′ (δ_C 133.3, Δδ 1.7), and C-2′ and C-6′ (δ_C 107.1, Δδ 0.1) (in acetone-d_6 + D_2O)] compared with those of **1**.[23] The symmetry of the B-ring was also demonstrated by the two-proton singlet observed at δ_H 6.60 (in acetone-d_6 + D_2O) in the ^1H NMR spectrum of **13**. The *Citrus unshiu* used in this experiment contained the 7-*O*-rutinosyl flavanones hesperidin and narirutin as major constituents, and **13** was probably produced by the same glycosidation mechanism. Based on these spectroscopic and chemical results, compound **13** was characterized to be (−)-epigallocatechin 4′-*O*-(6′-*O*-L-rhamnosyl)-β-D-glucoside (Fig. 3).

3. Conclusion

In this study, we demonstrated that the enzymes in the unripe fruit of *Citrus unshiu* can selectively oxidize pyrogallol-type catechins to produce dehydrotheasinensins. This selectivity represents a significant difference from the behaviors of most other plant homogenates, such as Japanese pear and loquat, which can oxidize both pyrogallol-type and catechol-type catechins to give the corresponding theaflavins and dehydrotheasinensins. Many plant homogenates have the ability to oxidize tea catechins to theaflavins and dehydrotheasinensins, even when the plants themselves do not contain polyphenols.[9] These enzymes only catalyze the transfer of electrons from catechins to oxygen molecules, and the reactions responsible for the formation of theaflavins and dehydrotheasinensins are therefore nonenzymatic reactions. This conclusion is supported by the fact that the enzymatic oxidation of **1** and **3** to dehydrotheasinensins was reproduced in a non-enzymatic stereoselective

oxidation reaction with $CuCl_2$.[8c] Furthermore, theaflavins can be produced by oxidation with $K_3[Fe(CN)_6]$.[3] The redox potential of pyrogallol-type catechins is much lower than that of the corresponding catechol-type catechins,[14] which is most likely related to the selective oxidation of pyrogallol-type catechins with the unripe fruit homogenate of *C. unshiu*. The enzymatic activity of the unripe fruit homogenate disappeared completely when the fruits were large (about 3 cm i.d.). This phenomenon is therefore very interesting from the perspective of plant physiology. Furthermore, we revised the structure of oolongtheanins, and proposed a new mechanism for their production. In oolong tea and black tea, oolongtheanins coexist with theasinensins. These two polyphenols are the oxidation and reduction products of dehydrotheasinensins, respectively, and are related to the oxidation‑reduction dismutation of dehydrotheasinensins.[13b,c] However, the yield of **11** (2.2%) was much lower than that of **8** (39%) in this experiment and many minor oxidation products of **5** were also observed, but remain uncharacterized. These products are probably related to uncharacterized black tea polyphenols.

4. Experimental section

4.1. Materials

(−)-Epigallocatechin was prepared from a commercial tea catechin mixture according to the methods described by Nonaka et al.[24] The resulting material was purified by crystallization from H_2O.

4.2. Analytical procedures

UV spectra were recorded on a Jasco V-560 UV/Vis spectrophotometer, and optical rotations were measured with a Jasco P-1020 digital polarimeter (Jasco, Tokyo, Japan). ^{1}H NMR, ^{13}C NMR, ^{1}H-^{1}H COSY, HSQC, and HMBC spectra were measured on a Varian UNITY plus 500 (500 MHz for ^{1}H; 125 MHz for ^{13}C) NMR spectrometer (Varian, Palo Alto, CA, USA), and a JEOL JNM-AL400 (400 MHz for ^{1}H; 100 MHz for ^{13}C) NMR spectrometer (JEOL, Tokyo, Japan). Coupling constants (*J*) are expressed in Hz and chemical shifts (δ) have been reported in ppm. FAB-MS experiments were conducted on a JEOL JMS-700N spectrometer (JEOL) using *m*-nitrobenzyl alcohol or glycerol as the matrix. Elemental analyses were conducted on a PerkinElmer 2400 II analyzer (PerkinElmer, Waltham, MA, USA). Column chromatography was performed using Diaion HP20SS (Mitsubishi Chemical, Tokyo, Japan), Sephadex LH-20 (25–100 μm; GE Healthcare Bio-Science, Uppsala, Sweden), and Chromatorex ODS (100–200 mesh; Fuji Silysia Chemical, Tokyo, Japan) columns. TLC was performed on precoated Kieselgel 60 F_{254} plates (0.2 mm thick; Merck, Darmstadt, Germany), using a 1:7:1 (v/v/v) mixture of toluene/ethyl formate/formic acid or a 14:6:1 (v/v/v) mixture of $CHCl_3$/methanol/H_2O as the solvent system. Spots on the TLC plates were visualized by UV illumination (254 nm) and by spraying the plate with 2% ethanolic $FeCl_3$ or 5% aqueous sulfuric acid reagent, followed by heating. Analytical HPLC was performed on a Cosmosil 5C_{18}-ARII column (250 × 4.6 mm i.d., 5 μm; Nacalai Tesque, Kyoto, Japan) with gradient elution from 4 to 30% CH_3CN in 50 mM H_3PO_4 over 39 min, followed by 30 to 75% CH_3CN in 50 mM H_3PO_4 over 15 min at a flow rate 0.8 mL/min. The column temperature was set at 35 °C, and the eluted compounds were detected with a JASCO MD-2010 photodiode array detector.

4.3. Oxidation of a catechin mixture using the plant homogenates

An aqueous solution was prepared containing (−)-epigallocatechin (**1**) (2.5 mg/mL, 8.2 μmol/mL), (−)-epicatechin (**2**) (0.6 mg/mL, 2.1 μmol/mL), (−)-epigallocatechin-3-*O*-gallate (**3**) (3.9 mg/mL, 8.5 μmol/mL), and (−)-epicatechin-3-*O*-gallate (**4**) (0.9 mg/mL, 2.0 μmol/mL). The proportion of the compounds used in the mixture was based on the concentrations found in Japanese green tea leaves. Unripe *Citrus unshiu* fruits (1.0–1.5 cm in diameter, 20 g) were homogenized with H_2O (20 mL) and Polyclar AT (2.0 g) in a Waring blender and filtered through filter paper (No. 2; Advantec, Tokyo, Japan). Samples (1.0 mL) of the catechin solution were placed in two test tubes, and they were treated with the homogenate (1.0 mL). The resulting mixtures were vigorously stirred for 1 h to entrain air/oxygen into the mixture. One of the reaction mixtures was then treated with ethanol (3.0 mL), and the resulting mixture was filtered through a membrane filter (0.45 μm) before being analyzed by HPLC. The other reaction mixture was heated with ascorbic acid (50 mg) at 90 °C for 10 min and then mixed with ethanol (3.0 mL). The resulting mixture was then filtered through a membrane filter (0.45 μm) before being analyzed by HPLC. Similar experiments were also performed using the Japanese pear fruit homogenate.

4.4. Oxidation of (−)-epigallocatechin (1) with the unripe fruit homogenate of *C. unshiu*

Several unripe *C. unshiu* fruits (100 g) were homogenized with H_2O (200 mL) and Polyclar AT (20 g) in a Waring blender and then filtered through filter paper under reduced pressure. The filtrate was

then treated with an aqueous solution of **1** (2.0 g/100 mL), and the resulting mixture was vigorously stirred for 1 h. The reaction was then stopped by the addition of ethanol (400 mL), and the resulting mixture was filtered. The filtrate was concentrated under reduced pressure at 40–45 °C and applied to a Diaion HP20SS column (60 × 5 cm, i.d.). The column was eluted with a mixture of H_2O and methanol (0–100%, 10% stepwise elution, each 500 mL) to give eight fractions: fr. 1 (1.8 g), fr. 2 (0.53 g), fr. 3 (0.78 g), fr. 4 (0.48 g), fr. 5 (0.21 g), fr. 6 (0.22 g), fr. 7 (0.27 g), and fr. 8 (0.43 g). HPLC and TLC analyses indicated that fractions 3 and 4 contained **8** and **1**, respectively, as the major components. Fraction 5 was purified on a Sephadex LH-20 column (0–100% methanol in H_2O) to give seven sub-fractions, and fr. 5-2 (25 mg) was purified on a Chromatorex ODS column (0–40% methanol in H_2O) to yield **13** (8.5 mg). Fraction 5-3 (63 mg) was purified on a Chromatorex ODS column (0–50% methanol in H_2O) to give compounds **8** (3.7 mg) and **1** (3.7 mg). Fraction 5-4 (27 mg) was subjected to a similar chromatographic process to that described above to give **12** (5.5 mg). Fraction 5-6 (33 mg) was identified as compound **11**. Fraction 6 was purified by column chromatography (Sephadex LH-20) to give nine sub-fractions. Fractions 6-6 (50 mg) and 6-8 (29 mg) were purified by column chromatography (Chromatorex ODS) to give compounds **12** (32.3 mg) and **11** (9.6 mg), respectively. Fraction 7 was also purified on a Sephadex LH-20 column to give seven sub-fractions. Fraction 7-6 (50 mg) was separated by column chromatography (Chromatorex ODS) to give **14** (17 mg). HPLC analysis of fr. 8 indicated the presence of hesperidin and narirutin, which exist in *C. unshiu* as major constituents. The total recovery of **1** was approximately 24%.

*4.4.1. Ethanol adduct **12**.* A tan amorphous powder, $[\alpha]_D$ +38.7° (*c* = 0.1, methanol). IR ν_{max} cm^{-1}:

3399, 1758, 1731, 1605, 1518, 1464, 1371, 1242. FABMS *m*/*z*: 655 $[M+H]^+$, 637 $[M–H_2O+H]^+$. Anal. Calcd for $C_{32}H_{30}O_{15}·4.5H_2O$: C, 52.25; H, 5.34; Found: C, 52.21; H, 5.09.

*4.4.2. (−)-Epigallocatechin 4′-O-(6′-O-L-rhamnosyl)-β-D-glucoside (**13**).* A brown amorphous powder, $[\alpha]_D^{26}$ +2.7° (*c* = 0.1, methanol). FABMS *m*/*z*: 615 $[M+H]^+$, 637 $[M+Na]^+$, 653 $[M+K]^+$. HRFABMS *m*/*z*: 615.1920 $[M+H]^+$ (Calcd. for $C_{27}H_{35}O_{16}$, 615.1925). IR ν_{max} cm^{-1}: 3393, 2932, 1627, 1516, 1464, 1362, 1275, 1196, 1145, 1063. UV (methanol) λ_{max} (log ε): 207 (3.76), 232 sh (3.27). ^{1}H NMR (CD_3OD, 400 MHz) δ: 6.58 (2H, s, H-2′, 6′), 5.93 (2H, s, H-6, 8), 4.80 (1H, br s, H-2), 4.73 (1H, d, *J* = 1.5 Hz, rha-1), 4.57 (1H, d, *J* = 7.8 Hz, glc-1), 4.21 (1H, m, H-3), 4.00 (1H, dd, *J* = 1.5, 10.7 Hz, glc-6), 3.87 (1H, dd, *J* = 1.5, 3.4 Hz, rha-2), 3.68 (1H, dd, *J* = 3.4, 9.8 Hz, rha-3), 3.62 (2H, m, glc-6, rha-5), 3.49 (2H, m, glc-2, glc-3), 3.42 (1H, t, *J* = 8.3 Hz, glc-4), 3.40 (2H, m, glc-5, rha-4), 2.86 (1H, dd, *J* = 4.4, 16.7 Hz, H-4), 2.73 (1H, dd, *J* = 2.7, 16.7 Hz, H-4), 1.25 (3H, d, *J* = 6.3 Hz, rha-6). ^{13}C NMR (CD_3OD, 100 MHz) δ: 157.1, 157.7, 158.0 (C-5, 7, 8a), 151.1 (2C, C-3′, 5′), 138.6 (C-4′), 133.8 (C-1′), 107.6 (glc-1), 107.3 (2C, C-2′, 6′), 102.5 (rha-1), 100.0 (C-4a), 95.9, 96.5 (C-6, 8), 79.6 (C-2), 77.7 (glc-3), 77.4 (glc-5), 74.9 (glc-2), 74.1 (rha-4), 72.3 (rha-3), 72.1 (rha-2), 71.4 (glc-4), 69.9 (rha-5), 68.2 (glc-6), 67.4 (C-3), 29.2 (C-4), 18.0 (rha-6). ^{1}H NMR (acetone-d_6 + D_2O, 400 MHz) δ: 6.60 (2H, s, H-2′, 6′), 5.99, 5.91 (each 1H, d, *J* = 2.2 Hz, H-6, 8), 4.83 (1H, br s, H-2), 4.74 (1H, br s, rha-1), 4.57 (d, *J* = 5.6 Hz, glc-1), 4.22 (br s, H-3), 4.00 (1H, m, glc-6), 3.88 (1H, m, rha-2), 3.67 (1H, dd, *J* = 3.4, 9.5 Hz, rha-3), 3.6–3.4 (overlapped with HOD signal, glc-2, 3, 4, 5, 6, rha-4, 5), 2.81 (1H, dd, *J* = 4.5, 16.7 Hz, H-4), 2.67 (1H, dd, *J* = 3.4, 16.7 Hz, H-4), 1.19 (3H, d, *J* = 6.1 Hz, rha-6). ^{13}C NMR (acetone-d_6 + D_2O, 100 MHz) δ: 157.45, 157.39, 156.5 (C-5, 7, 8a), 150.3

(2C, C-3′, 5′), 138.3 (C-4′), 133.3 (C-1′), 107.3 (glc-1), 107.1 (2C, C-2′, 6′), 101.8 (rha-1), 99.5 (C-4a), 96.1, 95.3 (C-6, 8), 78.9 (C-2), 77.0, 76.8 (glc-3, 5), 74.1, 73.3 (glc-2, rha-4), 71.9, 71.3, 70.7 (glc-4, rha-2, 3), 69.2 (rha-5), 67.8 (glc-6), 66.5 (C-3), 28.7 (C-4), 18.0 (rha-6).

*4.4.3. Acid hydrolysis of compound **13**.* Compound **13** (0.5 mg) was hydrolyzed with 0.5 M HCl (0.1 mL) in screw-capped vial at 100 °C for 3 h. The resulting mixture was neutralized with Amberlite IRA400 resin (OH^- form) and concentrated to dryness. The residue was dissolved in 0.1 mL of pyridine containing L-cysteine methyl ester (0.5 mL), and the resulting mixture was heated at 60 °C for 1 h. The mixture was then treated with a solution of *o*-tolylisothiocyanate (0.5 mg) in pyridine (0.1 mL), and the resulting mixture was heated at 60 °C for 1 h. The final mixture was then cooled to ambient temperature and directly analyzed by HPLC on a Cosmosil 5C_{18}-AR II column (250 × 4.6 mm i.d., Nacalai Tesque) at 35 °C. The column was eluted isocratically for 40 min with 25% CH_3CN in 50 mM H_3PO_4, and then washed with 90% CH_3CN in 50 mM H_3PO_4 at a flow rate 0.8 mL/min. The peaks at 16.91 and 28.01 min coincided with those of the thiazolidine derivatives of D-glucose and L-rhamnose (D-glucose 16.61 min; L-glucose 15.33 min; L-rhamnose 28.01 min; D-rhamnose 15.35 min). The retention time for the thiazolidine derivative of D-rhamnose was obtained from the product of the reaction of L-rhamnose with D-cysteine methyl ester.[22]

4.5. Calculations of ECD spectra and NMR chemical shifts

A conformational search was performed using the Monte Carlo method at the MMFF94 force field with Spartan′10 (Wavefunction, Irvine, CA, USA). The resulting low-energy conformers within

6 kcal/mol were optimized at the B3LYP-SCRF/6-31G(d,p) level (PCM). The vibrational frequencies were also calculated at the same level to confirm their stability, and no imaginary frequencies were found. The ^{1}H and ^{13}C NMR chemical shifts of the low-energy conformers with Boltzmann populations greater than 1% were calculated using the GIAO method at the mPW1PW91-SCRF/6-311+G(2d,p)//B3LYP-SCRF/6-31G(d,p) level in acetone (PCM).[20] The energies, oscillator strengths, and rotational strengths of the low-energy conformers were calculated using TDDFT at the CAM-B3LYP-SCRF/6-31G(d,p)//B3LYP-SCRF/6-31G(d,p) level in methanol (PCM).[17] The ECD spectra were simulated by the overlapping Gaussian function with a 0.3 eV exponential half-width. The calculated data for each conformer were averaged according to the Boltzmann distribution theory at 298 K based on their relative Gibbs free energies. All DFT calculations were performed using Gaussian 09.[25] GaussView was used to draw the molecular structures.[26]

4.6. Autoxidation of 3

A solution of **3** (100 mg) in 10% aqueous ethanol (100 mL) was mixed with phosphate buffer solution (pH 8.3, 500 mL), and the resulting mixture was held at 40 °C for 1 h. The reaction was then acidified (pH 4) by the addition of concentrated HCl, and the resulting solution was directly applied to a Diaion HP20SS column (20 × 2.0 cm), which was washed with water. The products adsorbed on the gel were subsequently eluted with 0–60% methanol (5% stepwise, each 50 mL) to yield galloyl oolongtheanin (**16**) (27.9 mg). All of the physical and spectroscopic data for **16** were identical to those reported previously.[5]

Acknowledgments

This work was supported by JSPS KAKENHI Grant Number 25870532. The authors are grateful to Mr K. Inada, Mr N. Yamaguchi, and Mr N. Tsuda (Center for Industry, University and Government Cooperation, Nagasaki University) for measurements of NMR, MS, and elemental analysis.

References and notes

1. Mai, V. C.; Bednarski, W.; Borowiak-Sobkowiak, B.; Wilkaniec, B.; Samardakiewicz, S.; Morkunas, I. *Phytochemistry* **2013**, *93*, 49–62.
2. (a) Haslam, E. *Phytochemistry* **2003**, *64*, 61–73; (b) Drynan, J. W.; Clifford, M. N.; Obuchowicz, J.; Kuhnert, N. *Nat. Prod. Rep.* **2010**, *27*, 417–462; (c) Li, S.; Lo, C.-Y.; Pan, M.-H.; Lai, C.-S.; Ho, C.-T. *Food Funct.* **2013**, *4*, 10–18.
3. Takino, Y.; Imagawa, H.; Horikawa, H.; Tanaka, A. *Agric. Biol. Chem.* **1964**, *28*, 64–71.
4. Nonaka, G.; Kawahara, O.; Nishioka, I. *Chem. Pharm. Bull*. **1983**, *31*, 3906–3914.
5. Hashimoto, F.; Nonaka, G.; Nishioka, I. *Chem. Pharm. Bull*. **1988**, *36*, 1676–1684.
6. Davis, A. L.; Lewis, J. R.; Cai, Y.; Powell, C.; Davis, A. P.; Wilkins, J. P. G.; Pudney, P.; Clifford, M. N. *Phytochemistry* **1997**, *46*, 1397–1402.
7. Haslam, E. *Practical Polyphenolics: From Structure to Molecular Recognition and Physiological Action*; Cambridge University Press: Cambridge, 1988; pp 138–177.
8. (a) Tanaka, T.; Matsuo, Y.; Kouno, I. *Int. J. Mol. Sci*. **2010**, *11*, 14–40; (b) Li, Y.; Tanaka, T.;

Kouno, I. *Phytochemistry*, **2007**, *68*, 1081–1088; (c) Shii, T.; Miyamoto, M.; Matsuo, Y.; Tanaka, T.; Kouno, I. *Chem. Pharm. Bull*. **2011**, *59*, 1183–1185.

9. Tanaka, T.; Mine, C.; Inoue, K.; Matsuda, M.; Kouno, I. *J. Agric. Food Chem*. **2002**, *50*, 2142–2148.

10. Fujita, S.; Tono, T.; Li, Z.-F. *Saga Daigaku Nogakubu Iho* **1990**, *68*, 9–15.

11. A preliminary study of the structural revision of oolongtheanins was reported: Tanaka, T.; Li, Y.; Matsuo, Y.; Shibahara, A.; Kouno, I. In *Polyphenols Communications 2010*, XXVth International Conference on Polyphenols, Montpellier, France, Aug 24-27, 2010; Ageorges, A., Cheynier, V., Lefer, P., Sarni-Manchado, P., Eds.; 2010; Vol.1, pp 165–166.

12. Yanase, E.; Sawaki, K.; Nakatsuka, S. *Synlett*, **2005**, 2661–2663.

13. (a) Tanaka, T.; Mine, C.; Watarumi, S.; Fujioka, T.; Mihashi, K.; Zhang, Y.-J.; Kouno, I. *J. Nat. Prod*. **2002**, *65*, 1582–1587; (b) Tanaka, T.; Watarumi, S.; Matsuo, Y.; Kamei, M.; Kouno, I. *Tetrahedron* **2003**, *59*, 7939–7947; (c) Matsuo, Y.; Tanaka, T.; Kouno, I. *Tetrahedron* **2006**, *62*, 4774–4783.

14. Roberts, E. A. H. *Chem. Ind*. **1957**, 1354–1355.

15. Nakai, M.; Fukui, Y.; Asami, S.; Toyoda-Ono, Y.; Iwashita, T.; Shibata, H.; Mitsunaga, T.; Hashimoto, F.; Kiso, Y. *J. Agric. Food Chem*. **2005**, *53*, 4593–4598.

16. (a) Gorin, P. A. J. *Can. J. Chem*. **1974**, *52*, 458–461; (b) Pfeffer, P. E.; Valentine, K. M.; Parrish F. W. *J. Am. Chem. Soc*. **1979**, *101*, 1265–1274.

17. (a) Nugroho, A. E.; Morita, H. *J. Nat. Med*. **2014**, *68*, 1–10; (b) Li, X.-C.; Ferreira, D.; Ding, Y.

Curr. Org. Chem. **2010**, *14*, 1678–1697.

18. (a) Tomita, I.; Sano, M.; Sasaki, K.; Miyase, T. In *Functional Foods for Disease Prevention I*; Shibamoto T., Terao J., Osawa T., Eds.; ACS Symposium Series 701; American Chemical Society: Washington, DC, 1999; pp 209–216. (b) Yoshino, K., Suzuki, M., Sasaki, K., Miyase, T., Sano, M. *J. Nutr. Biochem*.**1999**, *10*, 223–229. (c) Miyase, T.; Sano, M.; Nishimura, K. Jpn. Kokai Tokkyo Koho JP 1998130255 A 19980519, 1998.
19. Recently, a precursor of galloyl oolongtheanin (**16**) was reported: Hirose, S.; Tomatsu, K.; Yanase, E. *Tetrahedron Lett*. **2013**, *54*, 7040–7043.
20. (a) Lodewyk, M. W.; Siebert, M. R.; Tantillo, D. J. *Chem. Rev*. **2012**, *112*, 1839–1862; (b) Micco, S. D.; Chini, M. G.; Riccio, R.; Bifulco, G. *Eur. J. Org. Chem*. **2010**, 1411–1434; (c) Willoughby, P. H.; Jansma, M. J.; Hoye, T. R. *Nat. Protoc*. **2014**, *9*, 643–660.
21. Kazuma, K.; Noda, N.; Suzuki, M. *Phytochemistry* **2003**, *62*, 229–237.
22. Tanaka, T.; Nakashima, T.; Ueda, T.; Tomii, K.; Kouno, I. *Chem. Pharm. Bull*. **2007**, *55*, 899–901.
23. Davis, A. L.; Cai, Y.; Davies, A. P.; Lewis, J. R. *Magn. Reson. Chem*. **1996**, *34*, 887–890.
24. Nonaka, G.; Kawahara, O.; Nishioka, I. *Chem. Pharm. Bull*. **1983**, *31*, 3906–3914.
25. Frisch, M. J.; Trucks, G. W.; Schlegel, H. B.; Scuseria, G. E.; Robb, M. A.; Cheeseman, J. R.; Scalmani, G.; Barone, V.; Mennucci, B.; Petersson, G. A.; Nakatsuji, H.; Caricato, M.; Li, X.; Hratchian, H. P.; Izmaylov, A. F.; Bloino, J.; Zheng, G.; Sonnenberg, J. L.; Hada, M.; Ehara, M.; Toyota, K.; Fukuda, R.; Hasegawa, J.; Ishida, M.; Nakajima, T.; Honda, Y.; Kitao, O.; Nakai, H.;

Vreven, T.; Montgomery, J. A., Jr.; Peralta, J. E.; Ogliaro, F.; Bearpark, M.; Heyd, J. J.; Brothers, E.; Kudin, K. N.; Staroverov, V. N.; Kobayashi, R.; Normand, J.; Raghavachari, K.; Rendell, A.; Burant, J. C.; Iyengar, S. S.; Tomasi, J.; Cossi, M.; Rega, N.; Millam, M. J.; Klene, M.; Knox, J. E.; Cross, J. B.; Bakken, V.; Adamo, C.; Jaramillo, J.; Gomperts, R.; Stratmann, R. E.; Yazyev, O.; Austin, A. J.; Cammi, R.; Pomelli, C.; Ochterski, J. W.; Martin, R. L.; Morokuma, K.; Zakrzewski, V. G.; Voth, G. A.; Salvador, P.; Dannenberg, J. J.; Dapprich, S.; Daniels, A. D.; Farkas, O.; Foresman, J. B.; Ortiz, J. V.; Cioslowski, J.; Fox, D. J. *Gaussian 09*, Revision C.01; Gaussian, Inc.: Wallingford, CT, 2010.

26. Dennington, R.; Keith, T.; Millam, J. *GaussView*, Version 5.0.9; Semichem Inc.: Shawnee Mission, KS, 2009.